

Effect of Diagenetic Processes on Storage Capacity of Lower Miocene Rocks at Southwestern Sinai, Egypt

Nabil Aly Abd El-Hafez¹, Mohamed Wageeh Abd El-Moghny¹, Ahmed Salama Mousa², Tarek Youssef El-Hariri², Hossam El-Deen Khairy Hussein Sharaka³

1. Department of Geology, Faculty of Science, Al-Azhar University, Cairo, Egypt

2. Exploration Department, Egyptian Petroleum Research Institute (E.P.R.I.), Nasr City, Egypt

3. Regional Geology Department, Egyptian Geological Survey, Abbassiya, Cairo, Egypt

Abstract: The integrated petrographical and petrophysical examinations on selected samples at El-Markha and Wadi Gharandal sections, Southwestern Sinai, are carried out to determine the effect of diagenesis on the storage capacity of the Lower Miocene rocks (Nukhul and Rudeis formations). The microscopic examination of the clastic samples revealed that, the identification of six sandstone microfacies; quartz arenite, calcareous quartz arenite, ferruginous quartz arenite, glauconitic quartz arenite, ferruginous evaporitic quartz arenite and evaporitic quartz arenite. Carbonate rocks are represented by nine microfacies; sandy micrite, bio-sparite, foraminiferal bio-micrite, dolo-biomicrite, dolosparite, dolostone, pelsparite, oo-biosparite and evaporitic dolomicrite. The main diagenetic processes in different studied rock are cementation, neomorphism, glauconitization, replacement, dolomitization and dissolution. Porosity in the studied rocks is represented by primary (intergranular, intragranular and intercrystalline) and secondary types (intercrystalline, intragranular and channels porosity). The subsurface samples have lower porosity and permeability as well as storage capacity than surface studied samples, due to the forming of clay minerals in intergranular pores and the decreasing in grain size of the encountered quartz grains in subsurface samples.

Keywords: Diagenesis, Microfacies, Porosity, Permeability, Storage capacity, Miocene, Sinai, Egypt.

1-Introduction

The economically importance of the Miocene sedimentary rocks of Egypt increases with the continuous discoveries of oil and gas where these rocks can found as source, reservoir and cap rocks. The Miocene rocks in the Gulf of Suez and the Southwestern Sinai areas have attracted the attention of many authors (e.g., Moon and Sadek (1923), Tromp (1949), Ansary and Andrawis (1965), Said and El-Heiny (1967), Douban et al., (2002), Abd El-Rahman (2004), El-Azabi (2004), Mahran et al., (2007), Abul-Nasr et al., (2009), El-Bakry et al., (2010), Hewaidy et al., (2012), Al-Husseiny (2012). The syn-rift Miocene sediments that deposited in the failed rift basin have a rapid lateral variations in facies and thickness. These variations were influenced by the irregular palaeotopographic setting of the rift basin together with the continuous rising and sinking of the resultant sub-basin due to differential movements in pre-Cambrian basement blocks. Consequently, the Miocene sediments developed on the both rift shoulders and in the central sub-basins display two markedly contrast sedimentary facies, marginal and deeper marine. Deeper marine facies is marked by two major groups namely Gharandal and Ras Malaab. On the other hand, marginal marine facies is divided into four formations, from base to top; Abu Gerfan, Gharamul, Gamsa and Sarbut El- Gamal respectively (El-Azabi, 1997).

2-Stratigraphy

The encountered Miocene age in the Gulf of Suez region is proposed by the Stratigraphic Committee of Egyptian General Petroleum Corporation (E.G.P.C., 1964). The Lower Miocene in the Gulf of Suez and West Central Sinai is generally represented by two distinct facies, the marine facies and nonmarine or coastal facies. The variation of the environments is attributed to sea level changes that have been overprinted twice by two major tectonic movements; the mid-Rudeis and the post-Kareem event (Abul-Nasr et al., 1999). In the study area, the Lower Miocene is represented by marine facies of Gharandal group (Figs. 1&2).

The term of Gharandal Group was first mentioned by (Ghorab et al., 1964) to the rock unit overlies unconformably the Eocene limestones and conformably underlies Ras Malaab Group in the type locality at Wadi Gharandal surface section, Southwest Sinai. It is mainly composed of sandstones, shales, limestones with evaporites contaminations subdivided from base to top into; Nukhul, Rudeis and Kareem formations (N.S.S.C.G.S., 1974).

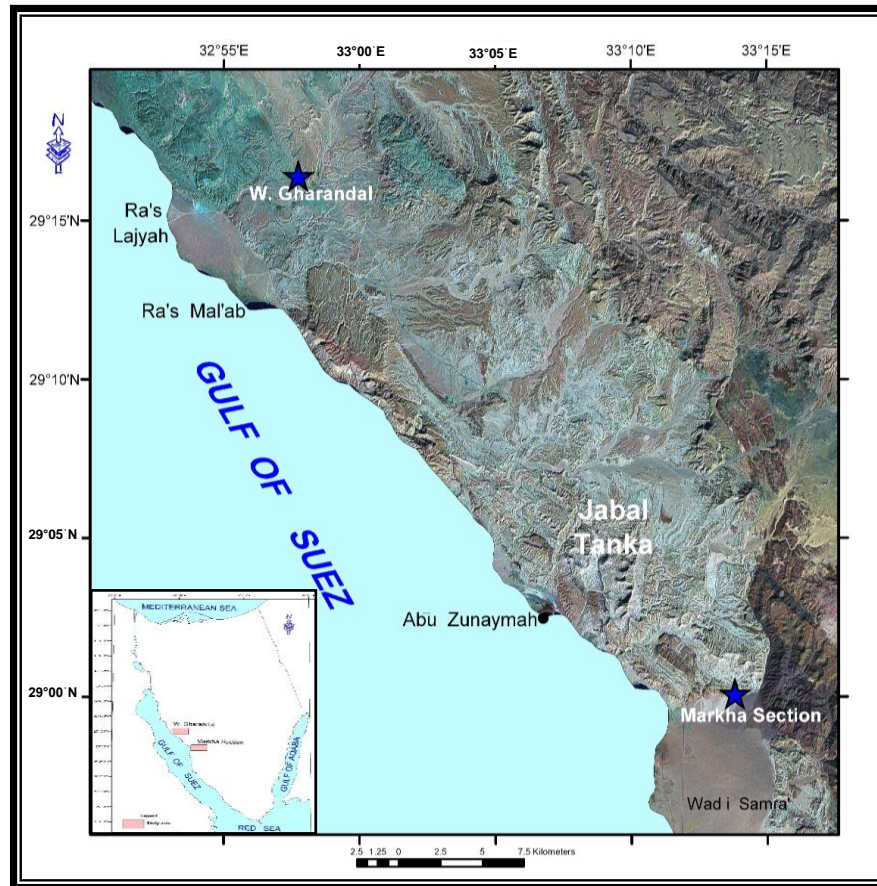


Fig. (1) Location map and landsat image of the studied sections

Nukhul Formation.

This formation was first described by (Waite and Pooley, 1953) in the type locality (Wadi Nukhul) and later adopted by the oil companies and accepted by (N.S.S.C.G.S., 1974). Nukhul Formation is subdivided in West Central Sinai by (Schlumberger well logs, 1989) into the following four informal members from base to top; Khoshera (upper shale), Nebwi (upper calcareous sandstone), Sudr (lower shale) and Ras Matarm (lower calcareous sandstone). These informal members represent alternating grey shale with calcareous sandstone and sandy limestones. Nukhul Formation marks the initial phase of early syn-rift marine invasion in the Gulf of Suez basin. It is unconformably overlies the Tayiba Red Beds (Upper Eocene) in El-Markha section and Tanka Formation (Middle-Upper Eocene) in Wadi Gharandal, (Fig. 3). The unconformity surface is represented by basal conglomerates that derived from the underlying rock units. Nukhul Formation unconformably underlies the Early Miocene Rudeis Formation and the unconformity surface is marked by the sharp facies change of post-Nukhul event, (Beleity, 1982). Nukhul Formation is related to Lower Miocene Aquitanian age, (Said and El-Heiny, 1967; Rateb, 1988, and Phillips et al., 1997).

Lithologically, Nukhul Formation in the studied sections is represented by limestones, sandstones and shales. Limestones are of grayish white to yellow color, massive, siliceous, hard, compact, dolomitic and fossiliferous lithofacies. Sandstones are yellow to reddish brown, compact, ferruginous, argillaceous with some salt intercalations. Shales are of yellow brown to grayish gray color, compact with veinlets of evaporites. Conglomerate thin beds in the lower part are made up of massive, grain-supported and polymictic texture consisting of reworked chert and carbonate clasts from the Eocene rocks. Conglomerate that attest to basin paleo-topographic irregularity caused by latest Oligocene-earliest Miocene tectonic activity (Early Clysmic event). Nukhul Formation is completely absent in South Gharib field indicating that the Western part of the studied area was still high during the deposition of the Nukhul Formation. The presence of relatively deep marine facies in the Eastern part of the studied area clearly indicates that the Miocene sea began to transgress from the North East, (Abd El-Hafez, 1986).

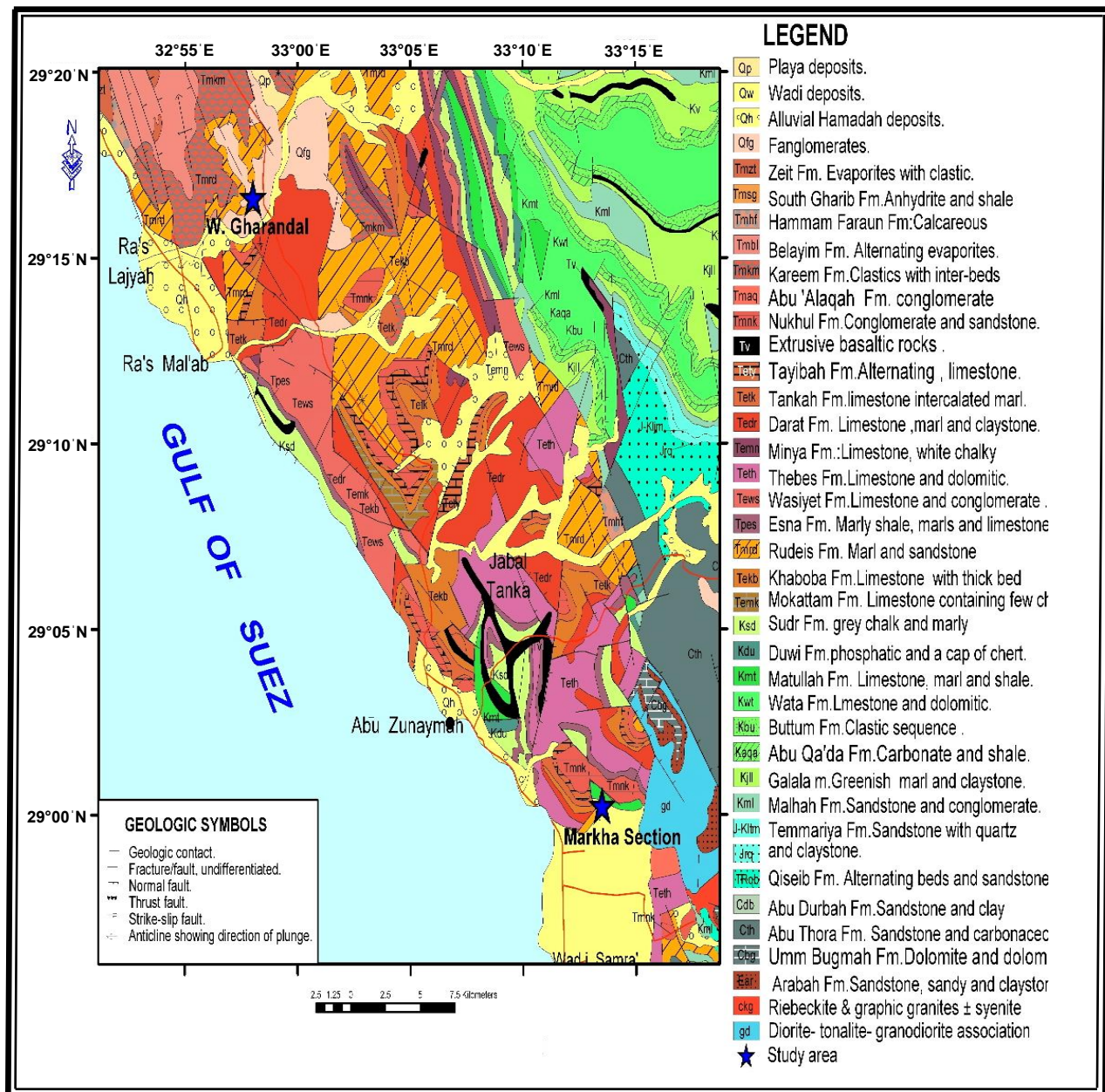


Fig. (2): Geological map of the studied sections (after Conoco, 1986).

Rudeis Formation

This formation was named by (Ghorab et al., 1964) and later adopted by the oil companies and accepted by (N.S.S.C.G.S., 1974) to represent sedimentary succession of shale, sandy shale, calcareous shale, calcareous sandstone and minor sandy limestone of Aquitanian-Burdigalian age, (Fig. 3). Rudeis Formation is made up of fine grained, highly fossiliferous shale with thin sandstone and limestone beds. It had deposited under open marine environment which periodically had subjected to warm semi-arid climate with high detrital input. This signifies an environmental shift from the shallow marine setting of Nukhul sediments towards a deeper one, due to increased rate in tectonic subsidence. It marks an abrupt change in lithology and faunal content from the underlying and overlying sediments, (El-Azabi, 2004).

Lithologically, Rudeis Formation is formed of shale, sandstone and limestones. Shale are varicolored (greenish brown, gray, yellowish gray, yellowish brown and light gray) silty, semi-compact, ferruginous, calcareous, laminated, highly fossiliferous and gypsum intercalations, Sandstones are characterized by yellowish to reddish brown color, semi-friable, ferruginous and gypsum veinlets. Limestones are of yellowish white color, hard, compact, ferruginous, dolomitic and fossiliferous lithofacies. Rudeis Formation unconformably overlies Nukhul Formation and unconformably underlies Kareem Formation. The lower unconformity is demarcated by sharp facies changes between the poorly fossiliferous Nukhul Formation and rich planktonic and benthic facies of the Rudeis Formation (El-Bakry et al., 2010). Facies aspect with high diversity and abundance microfaunal content of the Lower Rudeis Formation denote deposition in an open deep marine environment up to 200m water depth under warm semi-arid climate and during periods of high detrital input, (El-Azabi, 2004). The Rudeis Formation is subdivided from base to top into three informal members; Mheiherrat /Hawara, Asal and Mreir members, (N.S.S.C.G.S., 1974).

Mheiherrat/Hawara Member is composed of varicolored shale (yellowish gray to greenish brown), silty, semi-compact with veinlets of evaporites; yellowish white, hard, ferruginous limestone intercalations; sandstones, yellow to reddish brown, compact, ferruginous, argillaceous with some salt intercalations. This Member is unconformably overlies the Nukhul Formation by post-Nukhul event and unconformably underlie Asl Member by mid-Rudeis event.

Asl Member is made up of brownish gray, compact to semi-compact, silty, calcareous shale with gypsum veinlets and yellowish white, hard, fossiliferous limestone intercalations in the middle part.

Mreir Member consists of brownish yellow, compact, calcareous, ferruginous sandstone with some evaporites patches in the lower part and brownish yellow, hard, compact, siliceous, dolomitic limestone at the upper part. It is unconformably underlie Kareem Formation by post-Rudeis event.

Measured section

Two stratigraphic sections (El-Markha and Wadi Gharandal) have been measured, sampled and examined to determine their petrological and petrophysical characteristics. The obtained resulted are correlated with subsurface data in published works to recognize and interpret the differences of petrophysical characteristics between subsurface and studied exposed rocks. Field investigation established the vertical and lateral changes in lithology and sedimentary features of the different rock units (Figs. 1&3).

El-Markha section

This section is located between latitudes 29° 00` and 29° 03`N, and longitudes 33° 10` and 33° 16` E. The sedimentary succession of El-Markha section is represented by Nukhul and Rudeis formations and attains about (170m thick). Nukhul Formation (of about 100m thick) is unconformably capped by the Rudeis Formation which attains (70m. thick). Rudeis Formation overlain by Kareem Formation of Middle Miocene age.

Wadi Gharandal section

This section is located between latitudes 29° 14` and 29° 18` N, and longitudes 32° 55` and 33° 00` E. In Wadi Gharandal the Miocene succession is exposed at the both sides of the Wadi entrance. In this section, the sedimentary units measure about (325m thick). Nukhul Formation (ca. 90m thick) is unconformably overlain by the Rudeis Formation (Mheiherrat Member) which attains (235m. thick) and unconformably overlies Tanka Formation of Upper Eocene. Rudeis Formation unconformably capped by the Kareem Formation which are related to Middle Miocene age.

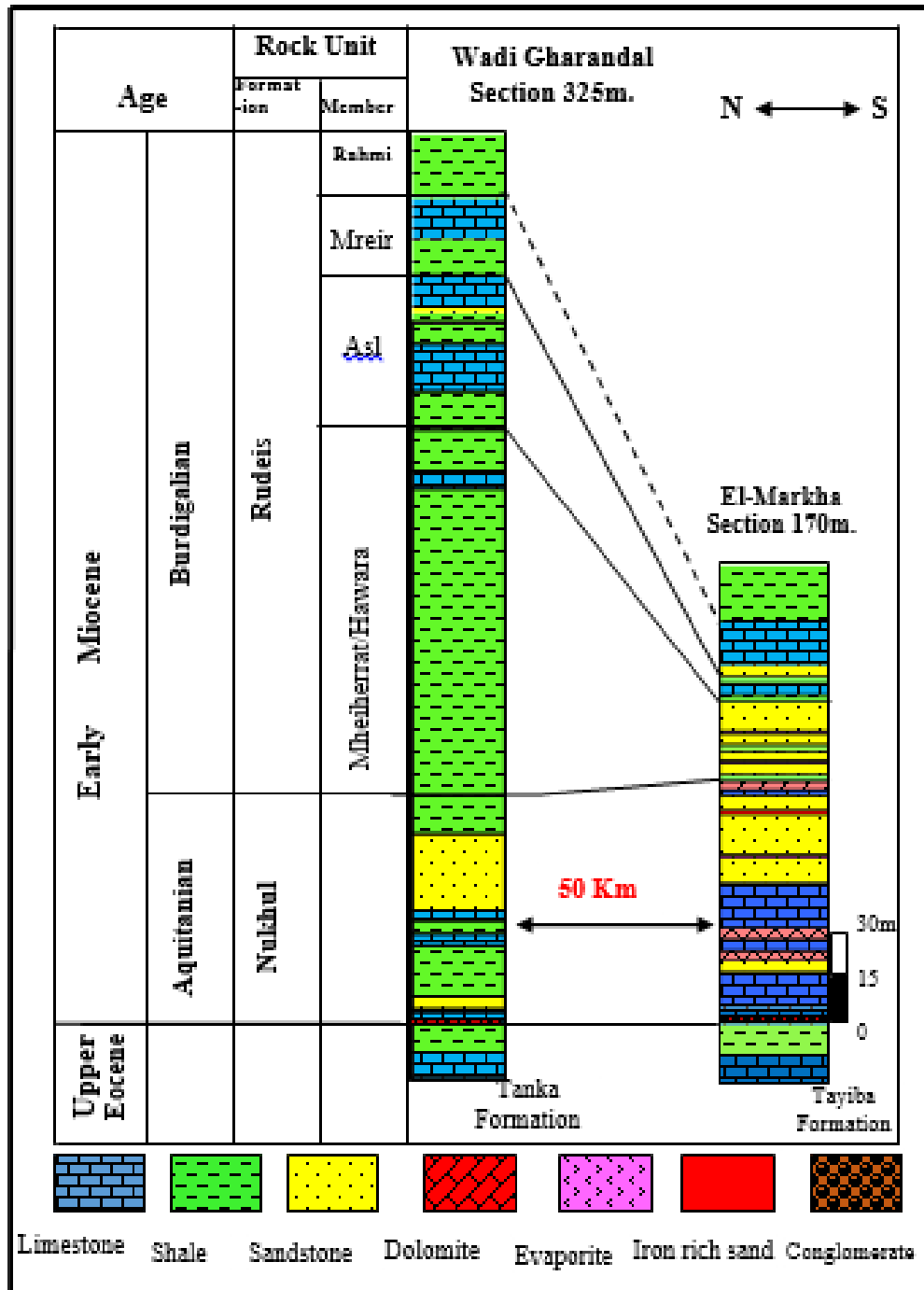


Fig. (3) Lithostratigraphic correlation of the Early Miocene rock units in studied sections.

3-Petrography

The microscopic study of the collected surface samples are carried out on 44 prepared thin sections to determine the petrographical characteristics of the Early Miocene rocks of Wadi Gharandal and El-Markha sections.

Petrography of Early Miocene clastic rocks

The petrographical studies are carried out on thirteen thin sections of the Early Miocene clastic rocks of Nukhul and Rudeis formations at El-Markha and Wadi Gharandal sections. The microscopic examination of these clastic samples revealed that, the identification of six microfacies types.

Quartz arenite

It is encountered only in the middle part of the Nukhul Formation at El-Markha section (Samples No. 12 & 14). This microfacies type consists of coarse to medium, sub-rounded to sub angular detrital quartz grains (95%) and about (5%) clay matrix, carbonate, evaporites and iron oxide cement (**Fig. 4-A**). Texturally, quartz grains are moderately to well sorted and most grains of monocrystalline and <7% of polycrystalline grains, and they are ranged from sub-mature to mature.

Glauconitic quartz arenite

This sandstone type is recorded in the middle and upper part of Nukhul Formation (Samples No. 11 & 18) and the Lower part of Rudeis Formation, Hawara Member (Sample No. 23). It consists of medium to coarse, sub-angular to sub-rounded, monocrystalline, moderately sorted, sub-mature detrital quartz grains forming about (80%) of the rock. These grains are cemented by argillaceous matrix. Glauconization observed as scattered grains or peloids, rounded to sub-rounded, green colored, may be formed from pre-existing clay minerals and/or by presence of decaying organic matter (**Fig. 4-B**).

Ferruginous quartz arenite

This microfacies is recorded in the upper part of the Nukhul Formation at El-Markha section (Samples No. 16, 17 and 19). It consists of medium to fine, sub-rounded to sub-angular, moderately sorted and sub-mature detrital quartz grains (52%). Few amount of evaporites mainly halite (4%) and argillaceous matrix can be noted. The intergranular pores are filled mostly by iron oxides cement mainly goethite and hematite (**Fig. 4-C**).

Ferruginous evaporitic quartz arenite

It is only encountered in the middle part of the Rudeis Formation at El-Markha section (Samples No. 29 & 30). It consists of coarse to medium sand size, sub-angular to sub-rounded, monocrystalline, moderately sorted and sub-mature detrital quartz grains forming about (75%) of the rock. These grains are cemented by iron oxide. Pores are filled mostly by iron oxide up to (10%) and evaporite mainly halite about (15%) (**Fig. 4-D**). This microfacies type is indicates to deposition under tidal flat zone.

Calcareous quartz arenite

This microfacies type is recorded in middle part of Nukhul Formation (Sample No. 15), and the upper part of Rudeis Formation, Asl Member at El-Markha section (Sample No. 34). It consists of coarse to medium sand size, moderately to well sorted, sub-angular to sub-rounded detrital quartz grains (about 65% of the rock) with some evaporites mainly halite about (11%) (**Fig. 4-E**). Some of these quartz grains are mostly monocrystalline and few are polycrystalline. Quartz grains are cemented by carbonate mainly (spary calcite crystals) about (20%).

Evaporitic quartz arenite

This microfacies is recorded in the lower part of the Rudeis Formation at El-Markha section (Sample No. 27). It consists of course to medium quartz grained. These grains are sub-angular to sub-rounded compose about (80%) of the rock (**Fig. 4-F**). Texturally, quartz grains are monocrystalline type, gray to pale yellow and colorless in color. Quartz grains are moderately to well-sorted, mature to sub-mature and cemented by evaporites mainly halite (*ca.*19%) with rare of iron oxide patches.

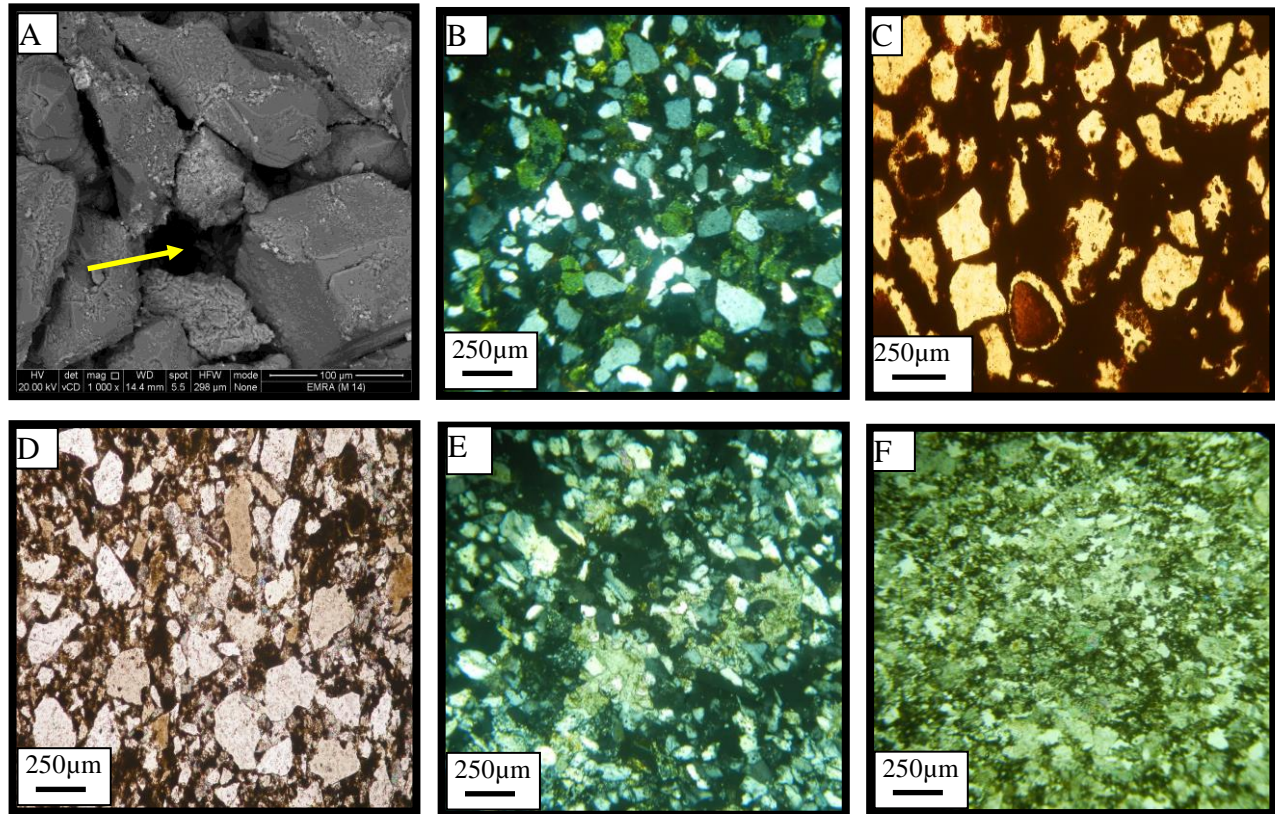


Fig. (4): photomicrograph showing different recorded sandstone microfacies (A) SEM of quartz arenite showing the intergranular porosity type (arrow); (B) glauconitic quartz arenite; (C) ferruginous quartz arenite; (D) ferruginous evaporitic quartz arenite; (E) calcareous quartz arenite; (F) evaporitic quartz arenite.

Petrography of Early Miocene non-clastic rocks

The classifications of [Folk \(1959, 1962, and 1974\)](#), [Dunham \(1962\)](#), and [Embry & Klovan \(1971\)](#) were used to identify the microfacies types of the studied carbonate rocks. The microscopic investigation of thirty one thin sections of carbonate samples of Nukhul and Rudeis formations in the studied sections are identified nine microfacies types.

Sandy micrite

It is recorded in the lower part of the Nukhul Formation at El-Markha section (Sample No. 1). This microfacies type is mainly consists of poorly fossiliferous cryptocrystalline calcite (micrite) groundmass (about 75% of the rock). It consists of medium to fine sand size and sub angular to sub-rounded detrital quartz grains about (15%). Some of dolomite rhombic crystals (10%) can be observed ([Fig. 5-A](#)). The subordinate spary calcite is due to the fact that no pore spaces in the micrite matrix were available.

Biosparite

This microfacies can be noted in the lower part of the Nukhul Formation (Sample. No. 2) and in the upper part of Rudeis Formation (Sample. No. 32) at El-Markha section. It consists of highly fossiliferous limestone and the allochems forming about (75%) of the rock. These bioclastic grains with a low diversity are represented by

echinoids shell fragments that scattered throughout microcrystalline spary calcite cement. The main diagnostic petrographic feature of echinoid fragments in this microfacies is synaxial overgrowth calcite cement (**Fig. 5-B**). Some grains about (3%) are fine to medium and angular to sub-angular detrital quartz grains. The carbonate grains have been heaped together by powerful currents persistent enough to winnow away any microcrystalline ooze that otherwise might have accumulated as a matrix. The interstitial pores have been filled by directly precipitated spary calcite cement.

Foraminiferal biomicrite

This microfacies is recorded in the lower part of the Nukhul Formation at El-Markha section (Samples No. 5, 9 and 10), and lower part of the Nukhul Formation at Wadi Gharandal section (Sample No. 1) as well as in the middle and upper parts of the Rudeis Formation at Wadi Gharandal (Samples. No. 34, 45, 47, 49, 50, 52, 53, 63, 64 and 65). It consists of planktonic foraminiferal tests (*ca.* 45%) embedded in a cryptocrystalline calcite (micrite) (up to 50% of the rock). Foraminiferal tests of different sizes can be noted and their chambers are filled by crystalline calcite cement while their walls are micritized (**Figs. 5-C**). The micrite matrix in samples (34, 45, 49 and 53) in Wadi Gharandal section form more than 80% of the rock. Few (3-4%) fine to medium grained, sub-angular to sub-rounded detrital quartz grains scattered throughout the calcite matrix. Spary calcite cement is present in a subordinate amount because no pore spaces were available for its formation in the micrite matrix and they partially fill the chambers of foraminiferal tests.

Dolo-biomicrite

This type of microfacies is encountered in the lower part of the Nukhul Formation at El-Markha section (Samples. No. 7&8). It consist of dolomite rhombs (15%), echinoid shell fragments about 10% with synaxial overgrowth cement. Bioclastic grains are embedded in cryptocrystalline calcite (micrite) matrix (up to 70% of the rock) (**Fig. 5-D**). Few (*ca.* 5%) shell fragments, which are filled with sparite, and iron oxide patches can be noted.

Dolo-sparite

This microfacies is detected in the upper part of the Rudeis Formation at El-Markha section (Samples No. 35&38) and consists of macrocrystalline calcite cement (sparite) about (66% of the rock) with clay matrix (up to 16%) and dolomite rhombus (about 14%). Texturally, dolomite crystals are of euhedral to subhedral (idiotopic to hypidiotopic) type. They are stained by iron oxide patches with reddish brown and dark brown color (**Fig. 5-E**).

Dolostone

This microfacies type is recorded in the lower part (Samples. No. 4&6) and in the upper part (Sample. No. 21) of Nukhul Formation at El-Markha section. It is composed of dolomite rhombs crystals (up to 58-85% of the rock) of meso to macrocrystalline. Texturally, dolomite crystals have sub-hedral to euhedral (idiotopic to hypidiotopic) shape (**Fig. 5-F**). Few dolomite crystals (2-7%) have an iron oxide stained zonation due to the mobility of oxidized ferrous iron from dolomite rhombs to the boundaries of the crystals. Spary calcite crystals well recorded in this microfacies although the majority of them have been dolomitized. Fine grained and angular to sub-angular detrital quartz grains about (2-5%) can be observed. Traces of shell fragments with their original structures can be noted while others are completely recrystallized into microspary calcite.

Pelsparite

This microfacies is observed in the middle part of the Nukhul Formation at El-Markha section (Sample. No. 20). It consists of carbonate peloids forming about 50% of the rock. Peloids are of spherical to oval shape, sized in 0.1-0.5 mm in diameter and composed of cryptocrystalline carbonate mud (micrite) without any internal structure (**Fig. 5-G**). Because pellets are soft when formed, they can be embayed or partially flattened by compaction during burial. These carbonate grains can be considered as fecal pellets. Some iron oxides patches can be noted (about 15%).

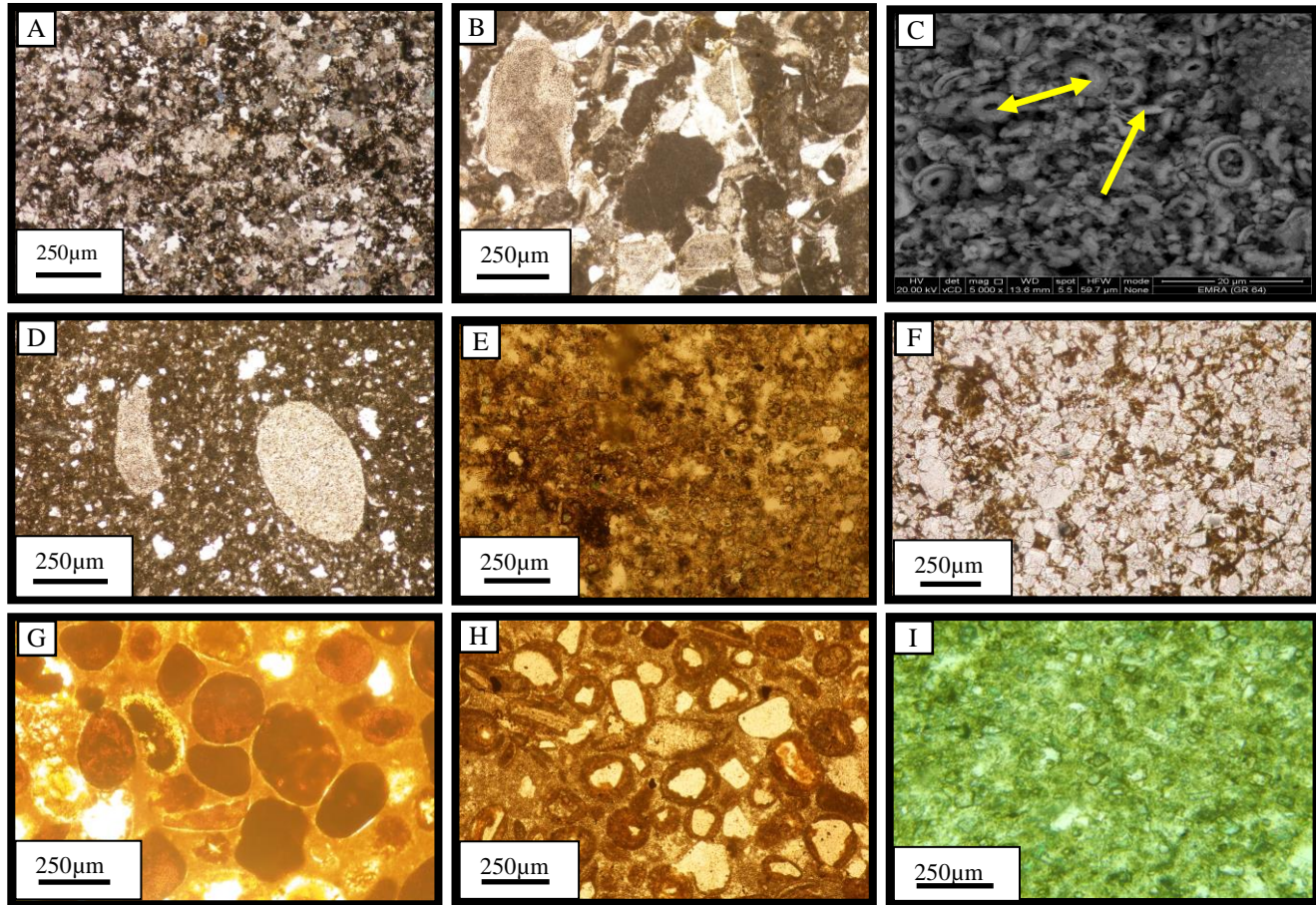


Fig. (5): photomicrograph showing different limestone microfacies types (A) sandy micrite; (B) biosparite; (C) SEM showing different types of porosity; the intergranular and intragranular porosity (arrows) within foraminiferal biomicrite microfacies; (D) dolo-biomicrite; (E) dolosparite; (F) dolostone; (G) pelsparite ;(H) oo-biosparite;(I) evaporitic dolomicrite

Oo-biosparite

This microfacies is noted in the upper part of the Rudeis Formation at El-Markha section (Samples No. 36&37). It consists of non-bioclastic carbonate grains (up to 45%) as ooids and shell fragments that embedded in microsparite groundmass (50-65% of the rock) (Fig. 5-H). Iron oxides patches of about (16-19%) can be observed. Ooids are spherical to subspherical grains, less than 2mm in diameter, and consisting of one or more regular concentric lamella around a nucleus (often a carbonate particle or quartz grain). The studied ooids thus favor normal marine environment of deposition, where the ooids are not broken.

Evaporitic dolomicrite

This microfacies is recorded in the lower part of the Nukhul Formation at Wadi Gharandal section (Sample No. 11). It consists of cryptocrystalline calcite matrix (micrite) (ca. 65% of the rock) and evaporite cement mainly halite about (21%). Few patches of sparitic calcite found as a result of recrystallization of micrite matrix (Fig. 5-I). Very fine dolomitic crystals are developed in this microfacies. Some of detrital quartz grained (<5%) can be noted as fine grained, rounded to sub-rounded, sub-angular grains. Iron oxides stain some grains with brown color.

4- Diagenesis

The type of diagenetic alteration depend upon the post-depositional environment while the degree of alteration is related to the duration of exposure to the environment (Purdy, 1968). El-Verhol and Groniles, (1981) discussed the effect of diagenesis on the physical properties of sedimentary rocks exposed at Sualbord region in Southern American and noted that the porosity increases due to less overburden, lower geothermal gradient reduced tectonic influence. They concluded that the depositional environment and fluid flow in addition to primary mineralogy are essential for diagenetic processes. Most diagenesis take place near the contact zone between two or three of the following phases, air, fresh water, sea water and sediment. Also the diagenesis and precipitation of cement is particularly active where two solution of different composition, temperature and CO₂ content are present (Khalial, 2004). The petrographical examination of thin section shows that the main identified diagenetic processes in the studied rocks are mentioned as the following:

Cementation

Cementation in sediments is the most important diagenetic processes leading to indurations of the loose sediments into rocks by precipitation of minerals from the interstitial fluids and/or forming authigenic minerals. It is a function of pressure, temperature, composition of the framework assemblage, composition of the solute, composition of pore water and time (Wood, 1989). One of the most porosity reducing process is cementation (Hayes, 1979). In the studied sandstone samples, cementation is represented by three kinds; the first is calcite (Figs. 4-E and 6) during early stage, the second is evaporites as (Figs. 4-F and 6) during late stage; finally, by iron oxides (Figs. 4-C, D and 6). The earliest authigenic mineral in the studied sandstone is hematite that occurs as rim on quartz grains. Hematite rims are commonly preserved between quartz grains and represent later authigenic phases. Iron could be supplied by intrastratal solution of ferrosilicate from the clayey beds present at the studied section since the diagenetic environment was oxidizing. The cementation process in the studied carbonate microfacies is clarified when the calcite cement take a form of mosaic cement and filling caves (Figs. 5-I and 7). These have been formed by selective solution of the lime-mud filling fossil molds and subsequent deposition of calcite during early diagenetic processes. The presence iron oxide as dispersed patches and cement in some carbonate samples reflects an oxidation condition accomplished with humid and arid condition resulting in deposition of iron oxide from pore water (Fig. 5-G&J and 7).

Neomorphism

The term "neomorphism" include all transformations between one mineral and it self or polymorph (Folk 1965). It is common in carbonate rocks with two aspects: the wet polymorphic transformation of aragonite to calcite and the wet recrystallization of cryptocrystalline calcite (micrite) to calcite cement. In the studied carbonate microfacies micrite is susceptible to diagenetic alteration and occasionally recrystallization to coarse mosaic of spars through aggrading neomorphism (Figs. 5-C, E, F, G, I and 7). This diagenetic process carried out during early stage of diagenetic processes (Priezbindowski 1985).

Glauconization

Glauconization observed as scattered grains or peloids, rounded to sub-rounded, green colored, may be formed from pre-existing clay minerals in warm water (15-200 C°) at depth range from 40 to 500m and under pH 7-8 (Figs. 4-B and 6). The formation of glauconite is facility by presence of decaying organic matter.

Replacement

This process involves the dissolution of the original minerals and growth of crystals of the replacing minerals as cement in both the formed and pre-existing void space (Blatt et al., 1972). Petrographical examination revealed the presence of iron minerals (hematite and goethite) in sandstone and (hematite) in carbonate samples (Figs. 4-C, D, 5-E, F, G, 6 and 7). Most of ferruginous cemented sandstone may have been originally formed by the oxidation of siderite (Pettijohn 1975). Walker et al. (1978) and Turner (1980) suggested that most of the hematite and its precursor oxides (mainly goethite) in sandstones have been formed in situ after deposition by the intrastratal alteration of iron bearing minerals in hot arid or semiarid climates or in

desert basin. The origin of iron oxides (hematite and goethite) is brought about by the seasonal lowering water tables and the development of well drained oxygenated conditions, allowing the oxidation of organic matter **Besly and Turner (1983) and Selley (1996)**. The oxidation of Fe^{2+} is more complete when the pH of solutions is relatively high (**Krauskopf, 1957**). The formation of iron oxides either as matrix or cement in intergranular pore spaces of the studied samples play a considerable role in reducing of porosity content.

Dissolution

The early diagenetic processes of studied sandstones include dissolution of certain framework of specific mineral as quartz. Dissolution in clastic rocks has been documented as an important diagenetic phenomenon in promoting secondary porosity (**Lundegard et al., 1984**) and increasing mineral maturity (**Abdel Wahab and McBride, 1991**), as well as texture maturity (**Walker et al., 1978**). It seems that the chemical characteristics of pore water were present in high temperature and alkalinity pH (>9) leading to dissolution of quartz grains. Quartz grains may be affected by acidic solution during early to middle stage and are corroded and etched to produce irregularly shaped grains (**Figs. 4-C, D and 6**). In contrast to that of sandstones, the dissolution is more common in carbonate rocks. It is the leaching of unstable minerals forming secondary pores, vugs, or caverns. All carbonate grains and cements exhibit dissolution features (**Montgomery, et al. 1998; Pratt, 2001 and El-Hariri, et al. 2007b**). Dissolution process produce most of the effective porosity. Moldic porosity is usually more pronounced than intergranular porosity. It occurred in several phases and all facies and cements were affected. Most of the ooids in oolitic sparite and foraminiferal biosparite microfacies were affected by an early and selective dissolution phase. Cement material is partially dissolved forming irregular longitudinal pores (channel porosity). This process led to development of medium to high porosity (**Figs. 5-B, C, E, H and 7**).

Dolomitization

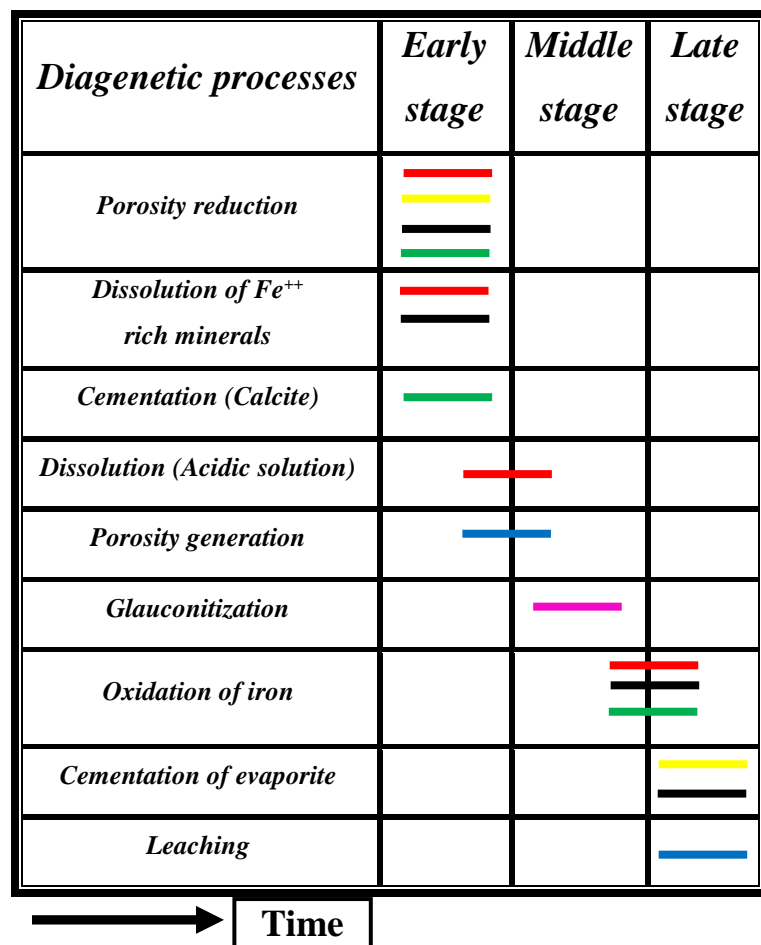
In the studied carbonate samples dolomitization process took place at the later stages after the sediments have been deposited and cemented. Transformation of calcite crystals to dolomite well developed in the studied samples (**Fig. 5-D, E, F, I and 7**). The conversion of smectite to illite, resulting in the release of free Mg, Ca and Fe ions forming probable source for the ferruginous, dolomitic and calcitic cement. Dolomitization is a diagenetic process due to chemical reaction between Mg-rich solution and solid $CaCO_3$ under acidic reduction medium (**Zenger, 1973**). This process plays a very important role in the development of secondary porosity and is considered as the main reason for the high porosity value. Dolomite has a more compact crystal structure than calcite so that theoretically the complete dolomitization of a limestone results in a porosity increase of 13%, as long as there is no subsequent compaction or cementation. In addition, dissolution of relict calcite in dolomitized limestone or increasing calcite dissolution relative to dolomite precipitation during the dolomitization process creates extra porosity (**Tucker, 2001**).

5-Reservoir characterization

The reservoir characterization of any hydrocarbon bearing system is dependent on its petrophysical parameters. These are (porosity, permeability, packing index, porosity ratio, fluid permeability, bulk density, grain density, and quality reservoir index....etc.) are of a great interest in reservoir studies. In the present work, thirty six samples were selected in El-Markha and Wadi Gharandal sections (26 and 10 respectively) to study the petrophysical properties and their relations to each other's and defining the best location with the higher storage capacity.

Petrophysical measurements

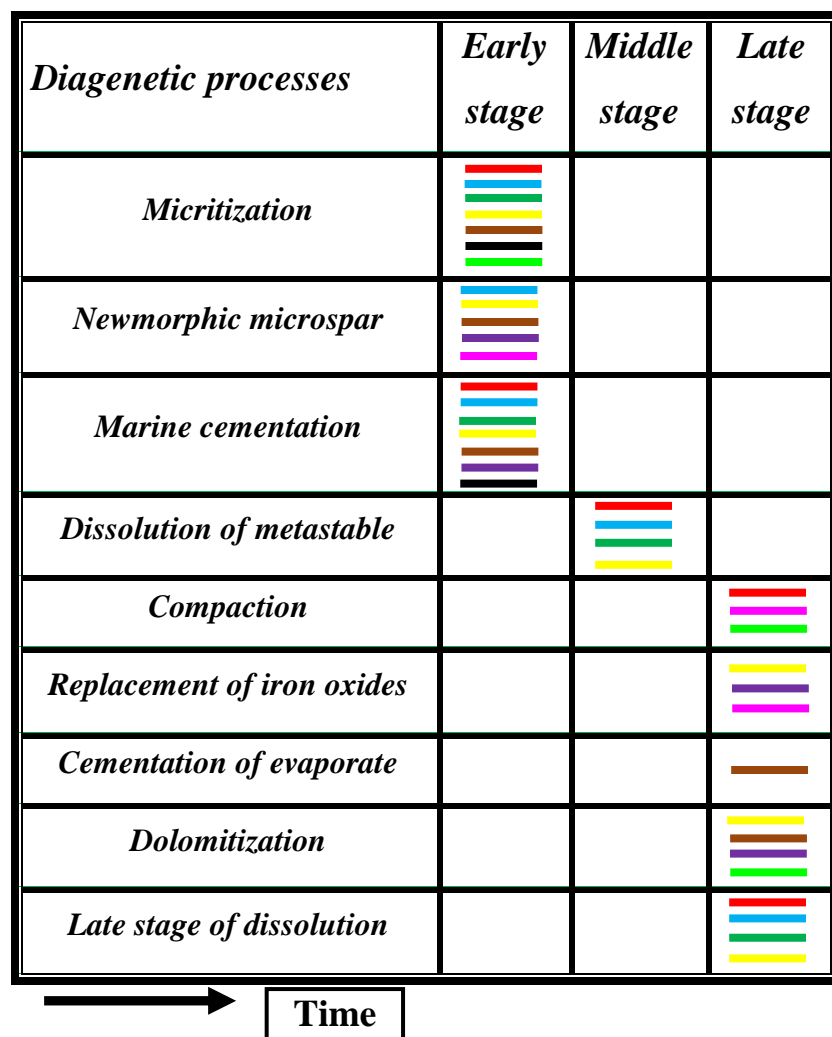
All of these samples have been subjected to Core-lab at the Egyptian Petroleum Research Institute (**E.P.R.I.**) using different methods to determine the: i) Density; ii) Porosity and iii) Permeability. The porosity is determined according to the methods of (**Rzhevsky et al., 1971; Kobranova, 1962; Dakhanova, 1977 and Ragab et al., 1985**), the permeability according to (**Leversone, 1967**). The packing index (Pi) is defined by **El Sayed (1993)**, porosity ratio defined by **Amaefule et al., (1993)**. The obtained results are correlated with published subsurface data (e.g., **El-Kadi et al., 2015**) of Lower Miocene rocks in Gulf of Suez. The vertical distribution of petrophysical parameters in selected samples are shown in (**Figs. 8 and 9**).



Legend

| Microfacies association | Symbol |
|---------------------------------------|--------|
| Quartz arenite | Blue |
| Ferruginous quartz arenite | Red |
| Evaporitic quartz arenite | Yellow |
| Ferruginous evaporitic quartz arenite | Black |
| Calcareous quartz arenite | Green |
| Glaucinitic quartz arenite | Pink |

Fig. (6): Diagenetic processes of studied sandstone samples at El-Markha and Wadi Gharandal sections.



Legend










| Microfacies association | Symbol |
|--------------------------|---|
| Biosparite |  |
| Foraminiferal biomicrite |  |
| Oo-biosparite |  |
| Dolosparite |  |
| Evaporitic dolomicrite |  |
| Dolostone |  |
| Sandy micrite |  |
| Pelsparite |  |
| Dolo-biomicrite |  |

Fig. (7): Diagenetic processes of studied carbonate samples at El-Markha and Wadi Gharandal sections.

Grain density (pb, gm /cc)

The petrophysical data of the studied samples (**Tables 1&2**) revealed that, the highest values of the grain density (3.00 gm/cm³) is recorded in the middle part of Nukhul Formation at El-Markha section which are represented by ferruginous quartz arenite (Sample No. 16) and lower part of Nukhul Formation at Wadi Gharandal section (2.69 gm/cm³) which are represented by argillaceous sandstone (Sample No. 3).

Table (1): Petrophysical parameters of the investigated samples of El-Markha section.

| Age | Formation | Member | Sample number | Grain density | Bulk Density | Porosity | Permeability | Packing index | Porosity ratio | QRI |
|---------------|-----------|--------|---------------|---------------|--------------|----------|--------------|---------------|----------------|------|
| Early Miocene | Rudeis | Mreir | M38 | 2.69 | 2.07 | 21.3 | 31.12 | 1.3 | 0.27 | 0.38 |
| | | | M37 | 2.7 | 2.06 | 22.1 | 33.6 | 1.31 | 0.28 | 0.39 |
| | | | M36 | 2.69 | 2.07 | 23.15 | 37.14 | 1.3 | 0.3 | 0.4 |
| | | | M35 | 2.69 | 2.04 | 22.7 | 34.4 | 1.32 | 0.29 | 0.39 |
| | | | M34 | 2.72 | 2.4 | 5.6 | 2.4 | 1.13 | 0.06 | 0.21 |
| | | Asl | M32 | 2.7 | 2.39 | 11.5 | 0.72 | 1.13 | 0.13 | 0.08 |
| | | Hawara | M30 | 2.34 | 2.12 | 4.8 | 0.23 | 1.1 | 0.05 | 0.07 |
| | | | M27 | 2.28 | 2.36 | 6.3 | 0.43 | 0.97 | 0.07 | 0.08 |
| | | | M23 | 2.31 | 1.87 | 17.3 | 2.7 | 1.24 | 0.21 | 0.12 |
| | Nukhul | | M21 | 2.91 | 1.97 | 32.6 | 0.64 | 1.48 | 0.48 | 0.04 |
| | | | M20 | 2.71 | 2.07 | 8.9 | 1.4 | 1.31 | 0.1 | 0.12 |
| | | | M19 | 2.7 | 2.19 | 4.3 | 0.95 | 1.23 | 0.04 | 0.15 |
| | | | M16 | 3 | 2.36 | 7.5 | 0.88 | 1.27 | 0.08 | 0.11 |
| | | | M15 | 2.71 | 2.08 | 9.2 | 0.67 | 1.3 | 0.1 | 0.08 |
| | | | M14 | 2.63 | 1.79 | 31.8 | 200.3 | 1.47 | 0.47 | 0.79 |
| | | | M12 | 2.65 | 1.97 | 25.6 | 40.1 | 1.35 | 0.34 | 0.39 |
| | | | M11 | 2.48 | 2.06 | 17 | 13 | 1.2 | 0.2 | 0.27 |
| | | | M10 | 2.58 | 2.1 | 18.9 | 1.6 | 1.23 | 0.23 | 0.09 |
| | | | M9 | 2.7 | 2.17 | 19.5 | 0.73 | 1.24 | 0.24 | 0.06 |
| | | | M8 | 2.75 | 2.1 | 23.5 | 0.45 | 1.31 | 0.31 | 0.04 |
| | | | M7 | 2.7 | 2.12 | 21.5 | 2.6 | 1.27 | 0.27 | 0.11 |
| | | | M6 | 2.84 | 2.3 | 19 | 0.71 | 1.23 | 0.23 | 0.06 |
| | | | M5 | 2.69 | 2.12 | 21 | 2.1 | 1.27 | 0.27 | 0.1 |
| | | | M4 | 2.71 | 2.24 | 17.7 | 5.5 | 1.21 | 0.22 | 0.18 |
| | | | M2 | 2.7 | 2.29 | 13.8 | 1.95 | 1.18 | 0.16 | 0.12 |
| | | | M1 | 2.77 | 2.28 | 17.8 | 0.01 | 1.21 | 0.22 | 0.01 |

Porosity (Φ)

The rock porosity is classified according to the mode of the origin (**Choquette and Pray, 1970 and Murray, 1990**) into primary and secondary porosity. The primary porosity is expressed as pores developed during the deposition of sedimentary rock. This porosity type well developed in the studied sandstone and carbonate samples as observed in petrographical and SEM analysis (**Figs. 4&5**). It is represented by structural pores such as intergranular, intragranular and intercrystalline pores in sandstones and carbonate facies.

Secondary porosity is formed after deposition as a result of some geologic processes such as: weathering, biological, deformation, fracturing, dolomitization, recrystallization as well as dissolution, leaching and removal of the dissolved material. The secondary porosity well developed in sandstone samples by leaching (**Fig. 4-A**), while in carbonate samples it is represented by dolomitization, recrystallization and dissolution (**Figs. 5-C, D, E, F and I**).

The obtained results from (Table 1) revealed that, the highest porosity values (31.8 and 32.6 %) *at El-Markha section* is recorded in Nukhul Formation (Samples No. 14 and 21 respectively) of quartz arenite and dolostone microfacies (Figs. 4-A and 5-F). These rocks had been affected by diagenetic processes such as porosity generation, leaching and dolomitization. *At Wadi Gharandal section*, the highest porosity value (33.7%) is recorded in (Sample No. 64) at Rudeis Formation, Asl Member (Table 2). This sample is described as foraminiferal biomicrite microfacies type. SEM and petrographical analyses reflect a great role of primary porosity (e.g. intergranular and intragranular pores) with effect of secondary porosity (e.g. channel) in this microfacies type (Fig. 5-C).

Table (2): Petrophysical parameters of the investigated samples of Wadi Gharandal section.

| Age | Formation | Member | Sample number | Grain density | Bulk Density | Porosity | Permeability | Packing index | Porosity ratio | QRI |
|---------------|-----------|--------|---------------|---------------|--------------|----------|--------------|---------------|----------------|------|
| Early Miocene | Rudeis | Asl | GR65 | 2.36 | 1.7 | 32.2 | 102 | 1.39 | 0.47 | 0.56 |
| | | | GR64 | 2.64 | 1.75 | 33.7 | 120 | 1.51 | 0.51 | 0.59 |
| | | | GR63 | 2.54 | 1.91 | 31.6 | 109 | 1.33 | 0.46 | 0.58 |
| | | | GR61 | 2.62 | 2.23 | 14.6 | 1.6 | 1.17 | 0.17 | 0.1 |
| | | | GR53 | 2.47 | 1.8 | 19.01 | 1.8 | 1.37 | 0.23 | 0.1 |
| | | | GR49 | 2.22 | 1.86 | 18.21 | 1.3 | 1.19 | 0.22 | 0.08 |
| | | | GR45 | 2.43 | 1.79 | 24.1 | 1.4 | 1.36 | 0.32 | 0.08 |
| | | Hawara | GR34 | 2.43 | 1.79 | 26.4 | 1.1 | 1.36 | 0.36 | 0.06 |
| | Nukhul | | GR11 | 2.51 | 2.29 | 5.3 | 1.2 | 1.1 | 0.06 | 0.15 |
| | | | GR3 | 2.69 | 2.58 | 3.8 | 0.9 | 1.04 | 0.04 | 0.15 |

Permeability (K, mD)

Permeability is a complex function of particle size, sorting, shape, packing and orientation of sediments. It is commonly defined as the ability of a medium to transmit a fluid (Boggs, 2009). The permeability of a rock is a measure of the ease with which fluid of a certain viscosity can flow through, it under a pressure gradient (Lynch, 1962 and Serra, 1984). It expressed in mille Darcy (mD).

The obtained results from (Table 1) reveal that, *at El-Markha section*, the highest values of permeability (200.3 mD) is recorded in middle part of Nukhul Formation (Sample No. 14) of quartz arenite microfacies type (Fig. 4-A). *At Wadi Gharandal section* (Table 2), the highest values (120 mD) are recorded in (Sample No. 64) which are represented by foraminiferal biomicrite microfacies type of Rudeis Formation, Asl Member (Fig. 5-C).

From the petrophysical studies we can reveal that, *El-Markha section*, Nukhul Formation (Samples No. 12&14) and *Wadi Gharandal section*, Rudeis Formation (Samples No. 63, 64 and 65) are characterized by high porosity and permeability values associated with decrease in the grain and bulk density. Whatever, the quality reservoir index, packing index and porosity ratio increase when the porosity and permeability increase. Petrophysical properties (porosity, permeability, packing index, porosity ratio, fluid permeability, bulk density, grain density, and quality reservoir index etc.) have a great role in defining the best location with the high storage capacity.

Vertical distribution of different petrophysical parameters in El-Markha and Wadi Gharandal sections,

From vertical distribution of the different petrophysical parameters in El-Markha and Wadi Gharandal sections reveal that, the middle part of Nukhul Formation, **El-Markha section**, (Samples No. 12, 14) which represented by quartz arenite microfacies are composed of quartz arenite with well sorted, very coarse to coarse sand grained. These zone have a high porosity (31.8 %) and permeability (200.3mD) values, and affected by leaching process during late stage of diagenetic process. The porosity ratio, packing index, and quality reservoir index increasing with increases porosity and permeability, as well as decreasing in the grain and bulk density (These zone represented best place as a good storage capacity).

Meanwhile, the upper part of Rudeis Formation (Samples No. 35, 36, 37 and 38) which represented by Oo-biosparite and dolosparite microfacies which affected by micritization, marine cementation, dolomitization and dissolution processes, characterized by good porosity, permeability, packing index, porosity ratio and quality reservoir index associated with decrease in the grain and bulk density as well as good storage capacity (**Fig. 8**). On the other hand, **Wadi Gharandal** section in the upper part of Rudeis Formation (Samples No. 63, 64 and 65) which represented by Foraminiferal biomicrite microfacies type characterized by high porosity, permeability, porosity ratio, packing index and quality reservoir index associated with decrease in the grain and bulk density as well as best place as a good storage capacity. Also, the upper part of Rudeis Formation (Samples No. 34, 45, 49, 53 and 61) which are represented by Foraminiferal biomicrite microfacies types characterized by high porosity and fair permeability, porosity ratio, packing index and quality reservoir index associated with decrease in the grain and bulk density due do presence of authigenic clay minerals (**Fig. 9**).

Subsurface well log data classified Nukhul Formation into four net pay zones (**A, B, C and D**). Their zone (C) has a higher porosity content (13-21%) than other identified zones. It is made up of sub-angular to sub-rounded, moderately sorted and fine to very fine-sand quartz grains. Authigenic clay minerals (e.g. glauconite and kaolinite) and K-feldspars can be detected in subsurface samples by microscopic examination. The reducing of porosity values in the subsurface data due to the forming of clay minerals in intergranular pores and the decreasing in grain size of the encountered quartz grains (**El Kadi et al., 2015**). The development of authigenic clay minerals within the pore spaces as a result of interaction between the pore-water and detrital grains or by direct precipitation from the pore water could destroy the primary porosity and decrease permeability (**Jonas and McBride, 1977**).

The recorded ferruginous quartz arenite in upper part of Nukhul Formation at **El Markha section** has slightly low porosity (4.3-7.5%) and permeability (0.88-0.95 mD) values that may duo to the formation of authigenic iron minerals (hematite and goethite) and filling the intergranular pores as observed in petrographical studies (**Fig. 4-C&D**). Also, the detected evaporitic sandstone types have low porosity (6.3%) and fair permeability (0.43 mD) values as a result of evaporite precipitation in intergranular pores (**Fig. 4-D&F**). The examined dolostone microfacies in upper part of Nukhul Formation has a high porosity value (32.6%) with fair permeability (0.64 mD) duo to the precipitation of authigenic iron minerals (goethite) which are detected by petrographical study (**Fig. 5-F**). Dolosparite and/or oo-biosparite microfacies of upper part from Rudeis Formation are characterized by good porosity (21.3-23.15%) and permeability (31.12-37.14 mD) values (**Table 1**) duo to the dolomitization effect. **At Wadi Gharandal section**, the foraminiferal biomicrite microfacies of upper part of Rudeis Formation are characterized by high porosity (33.7%) and permeability (120 mD), which are represented by primary and secondary types (intergranular, intragranular and channels) as recorded in petrographical and SEM analysis (**Table 2**).

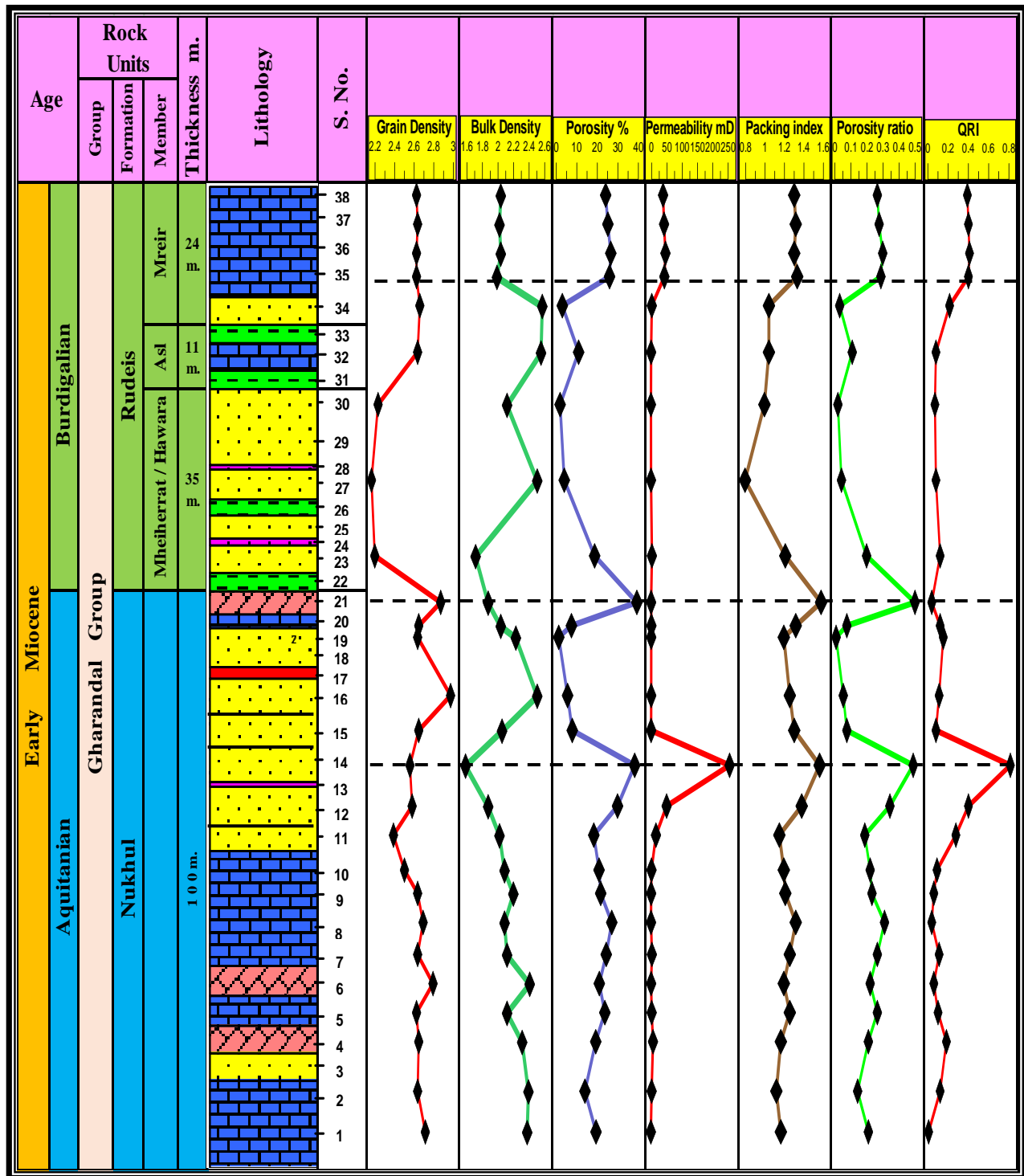


Fig. (8): Vertical distribution of the petrophysical properties at El-Markha section.

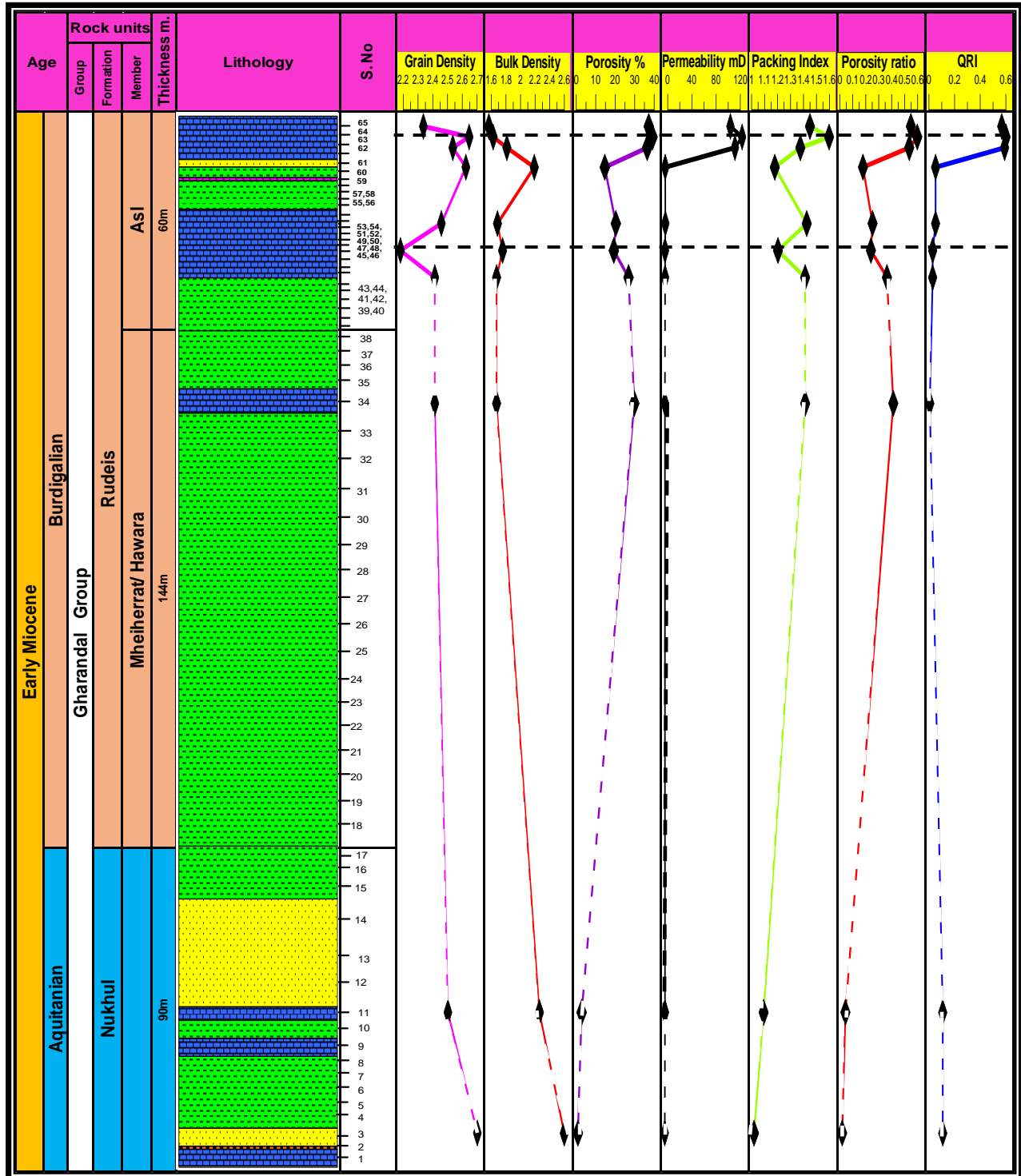


Fig. (9): Vertical distribution of the petrophysical properties at Wadi Gharandal section.

6-Conclusion

The Lower Miocene rocks in the studied sections can be classified into clastic (sandstones and argillaceous) and non-clastic (carbonate rocks with thin evaporitic intercalations). The microscopic examination revealed different sandstone microfacies types such as; quartz arenite, calcareous quartz arenite, ferruginous quartz arenite, evaporitic quartz arenite, glauconitic quartz arenite and ferruginous evaporitic quartz arenite. The carbonate microfacies types in the studied formations include sandy micrite, biosparite, foraminiferal biomicrite, dolo-biomicrite, dolosparite, dolostone, pelsparite, oo-biosparite and evaporitic dolomicrite. The diagenetic processes act the major role in storage capacity of the studied Lower Miocene rocks. Cementation, neomorphism, glauconitization and replacement as diagenetic processes resulted in formation of authigenic and cement minerals in pore spaces and decrease the porosity and permeability values in the studied rocks. On the other hand, dolomitization, leaching and dissolution increase the porosity, permeability values and therefore the storage capacity in carbonate and sandstone samples. From the obtained petrophysical results it can conclude that quartz arenite sandstone types of middle part of Nukhul Formation at El-Markha section (Samples No. 12&14) and foraminiferal bio-micrite microfacies of Rudeis Formation, Asl Member (Samples No. 63, 64 and 65) at Wadi Gharandal section represented the best place as a good storage capacity.

References

- Abd El-Hafez, N.A.M. (1986):** Evaluation of Petroleum Prospect of some areas in the Gulf of Suez region. Ph.D. Thesis, geology department, Al-Azhar University, A.R.E. Cairo, Egypt. p. 384.
- Abd El-Rahman, A.Y.A. (2004):** Petrophysical Characteristics of Nukhul Formation, Northern Part of the Gulf of Suez, Egypt. Bull. Net, Res, Cent, Cairo, Egypt. Vol. 29, No.4, pp. 441-463.
- Abd El-Wahab, A.A. and McBride, E.F. (1991):** Diagenetic control or reservoir quality of Araba and Naqus diagenetic quartz arenites (Cambrian), Gebel Araba-Qabeliat, Southwest Sinai, Egypt. Egyptian Delta J. Sci., 15, pp. 160-203.
- Abul-Nasr, R.A., and Salama, G.R. (1999):** Paleoecology and depositional environments of the Miocene rocks in Western Sinai, Egypt. M.E.R.C., Ain Shams Univ., Earth Sci. Ser., Vol. 13, pp. 92-134.
- Abul-Nasr, R.A., El-Safari, Y.A., Attia, S.H. and Maih, A. (2009):** Stratigraphy and depositional settings of the Miocene succession in the area between Wadi Sudr and Wadi Wardan, Gulf of Suez region. Egyptian Jour. of Paleontol. Vol. 9, pp. 119-144.
- Al-Husseiny, M.I. (2012):** Late Oligocene-Early Miocene Nukhul Sequence, Gulf of Suez and Red Sea. Geo. Arabia, Vol. 17, pp. 17-44.
- Amaefule, J.O., Altunbay, M., Tiab, D., Kersey, D., and Keelan, D.K. (1993):** Enhanced reservoir description, using core and log data to identify hydraulic (flow) units and predict permeability in un-cored intervals/ wells SPE-26436, Society of Petroleum Engineers Conference, Houston, Texas, U.S.A., 3-6 October, pp. 94-135.
- Ansary, S.E., and Andrawis, S.E. (1965):** The Miocene biostratigraphy of the Rahmi-shukheir area, Eastern Desert, Egypt, U.A.R. Proc. 5th Arab Petr. Congr., Serial No.33 (B-3), pp. 1-8.
- Beleity, A. (1982):** "The composite standard and definition of paleo-events in the Gulf of Suez". 6th E.G.P.C., Exploration Seminar, Cairo, Egypt, pp. 181-189.
- Besly, Y.B. and Turner, P. (1983):** Origin of red beds in a moist tropical climate (Etruria Formation, Upper Carboniferous, UK). In: Wilson, R.C. (ed.) Residual Deposits: Surface Related Weathering Processes and Materials. Geol. Soc. London Spec. Publ., 11, p. 131.
- Blatt, H., Middleton, G. and Murray, R.C. (1972):** Origin of sedimentary rocks. Prentice Hall, New Jersey, p. 500.
- Boggs, J.R., (2009):** Petrology of sedimentary rocks. 2nd edition, Cambridge University Press. U.S.A., New York, pp. 59-62.

- Choquette, P.W., and Pray, L.C. (1970):** Geological nomenclature and classification of porosity in sedimentary carbonates. A.A.P.G., pp. 207-250.
- Conoco. (1986):** Geological map of Egypt, Scale 1:500.000, 6 Sheets, with cooperation of Egyptian General Petroleum Corporation, Klitzsch, E., List, F.K. and Pohlmann, G. (Editors), Berlin, Cairo, Egypt.
- Dakhanova, N.V. (1977):** Determination of the petrophysical characteristics of sample in Russian. Nedra. Moscow. p. 41.
- Dunham, R.J. (1962):** Classification of carbonate rocks according to depositional texture. Bull. A.A.P.G., Tulsa / Oklahoma. Mem. (1), pp. 108-121.
- Egyptian General Petroleum Corporation (E.G.P.C.) (1964):** Oligocene and Miocene rock stratigraphy of the Gulf of Suez region. Report of the Stratigraphic Committee, p. 142.
- El-Azabi, M.H. (1997):** The Miocene marginal marine facies and their equivalent deeper marine sediments in the Gulf of Suez, Egypt: A revised stratigraphic setting. Egypt. J. Geol., Vol. 41(2A), pp. 273-308.
- El-Azabi, M.H. (2004):** Facies characteristics, Depositional styles and evolution of the syn-rift Miocene sequences in Nukhul-Feiran area, Sinai side of the Gulf of Suez rift basin, Egypt. Geol. Dept. Bldg., Fac. Sciences, Ain Shams Univ. Cairo. Sedimentology of Egypt. Sediment. Soc. Vol. 12, pp. 69-103.
- El-Bakry, H.M., Zahra, H.A., Khater, T.M., Fawwaz, S.E., and Almoazamy, A.A. (2010):** Geology of West Central Sinai, Egypt. Geol. Surv. Unpublished Report No. 53, p. 44-48.
- El-Hariri, T.Y., Mousa, A.S. and Ibrahim, G. El-Din. (2007b):** Diagenetic processes, geochemistry and petrophysical properties of the Upper Cretaceous Matulla and Thelmet formations at Wadi El Ghaib, South-eastern Sinai, Egypt. Aust. J. of Bas. And Appl. Sci., 1(4). pp. 487-496.
- El-Kady, H.H., Ahmed S.S. Ahmed., M. F.M. and Taher, M.T.M. (2015):** Core-Log Integrated Formation Evaluation and Application of Flow unit Concept at Rudies-Sidri Field, Gulf of Suez, Egypt. International Journal of Innovative Science Engineering Technology, Vol. 2, issue: 8, August. pp. 615-630.
- El-Sayed, A.M.A. (1993):** Packing index and saturation parameters for limestone, Ain Shams Sci., Bull. Vol. 31, pp. 411-424.
- El-Verhol, A., and Groniles, G. (1981):** Diagenetic and sedimentology explanation for high seismic sediment, Sualbord Region. A.A.P.G., Bull., Vol. 65/1, pp. 145-153.
- Embry, A.F. and Klovan, J.E. (1971):** Absolute water depth limits of Late Devonian paleontological zones. Geol. Rundschau, 61, pp. 672-686.
- Folk, R.L. (1959):** practical petrographic classification of limestone. A.A.P.G., Tulsa / Oklahoma, Bull. Vol. 43, pp. 1-38.
- Folk, R.L. (1962):** Spectral subdivision of limestone type. In. HAMED, W. E. (Ed): Classification of carbonate rocks. A.A.P.G., Tulsa / Oklahoma, Men, 1, pp. 62-84.
- Folk, R.L. (1965):** Some aspects of recrystallization in ancient limestone. In. (L.C. Pray and R.C. Murray Eds.) Dolomitization and limestone diagenesis. Soc. Econ. Paleont. Min. Spec. Publ. (13), pp. 1-48.
- Folk, R.L. (1974):** Petrography of sedimentary rocks. Notes, Hemphill publ. Eo. Drawer M. Univ. station, Austin Texas, p. 174.
- Ghorab, M.A. and Marzouk, I. M. (1964):** A Summary Report on the Rock Stratigraphic Classification of the Miocene non-Marine and Coastal Facies in the Gulf of Suez and Red Sea Coast (unpublished report, E.R.601).
- Hayes, J.B. (1979):** Sandstone diagenesis, the hole truth. SEPM Spec. Publ., 26, pp. 127-139.
- Hewaidy, A.A., Farouk, S., and Ayyad, H.M. (2012):** Nukhul Formation in Wadi Baba, Southwest Sinai Peninsula, Egypt. Gulf Petro Link, Bahrain, Geo Arabia, Vol. 17, no. 1, pp. 103-120.
- Jonas, E.C., and McBride, E.F. (1977):** Diagenesis of sandstone and shale: application to exploration for hydrocarbons; Dept. Geol. Sci., Univ. Texas, Ausin, Cont. Educ. Prog. Publ. No.1.

- Khalial, M.H. (2004):** Petrology and geochemistry of the Turonian sedimentary sequence in Southern Sinai, Egypt. Ph.D. Theses. Al- Azhar Univ., Cairo, Egypt, p. 274.
- Kobranova, V.N. (1962):** Physical properties of rocks. In Russian Gestepechizdat, Moscow, p. 490.
- Krauskopf, K.B. (1957):** Separation of manganese from iron in sedimentary processes. Geochem. ET. Cosmochem Acta. V.12, pp. 61-84.
- Liversone, A.I. (1967):** Geology of Petroleum. C.B.S Publishers and Distribution, pp. 77-137.
- Lundegard, D., Land, L.S. and Galloway (1984):** Problem of secondary porosity: Frio Formation (Oligocene). Texas, Gulf Coast. Geology, 12, pp. 399-402.
- Lynch, E.J. (1962):** Formation evaluation. Harper and Row, Publishers, New York, p. 422.
- Mahran, T.M., El-Haddad, A.A., and Hassan, A.M. (2007):** Facies and Sequence Stratigraphy of the Syn-Rift Miocene Mixed Carbonate Siliciclastic Sediments of Sidri-Feiran area, Southwest Sinai, Egypt; Bull. Fac. Sci., Zagazig Univ., V. 29, pp. 355-406.
- Montgomery, S.L., and Dixon, W.H. (1998):** New depositional model improves outlook for clear Fork infill drilling: Oil and Gas Journal, V.96, pp. 94-98.
- Moon, F.M., and Sadek, H. (1923):** Preliminary Geological Report on Wadi Gharandal Area. Western Sinai, Egypt, (Petrol. Research ser.), Bull. No. 12, p. 42.
- Murray, R.C. (1990):** Origin of porosity in carbonate rocks. Jour. Sed. Petrology, V. 30, pp. 59-84.
- National Stratigraphic Sub-Committee of the Geological Science of Egypt "N.S.S.C.G.S." (1974):** Miocene rock stratigraphy of Egypt., Egypt. J. Geol., Vol. 18, pp. 1-59.
- Pettijohn, F.J. (1975):** Sedimentary rocks. Harper and Row. New York, 3rd ed., p. 628.
- Phillips, G., Imam, M.M., and Abdel Gawad, G.I. (1997):** Planktonic foraminiferal biostratigraphy on the Miocene sequence in the area between Wadi El-Tayiba and Wadi Sidri, west central Sinai, Egypt: Journal of African Earth Sciences, Vol. 25 (3), pp. 435-451.
- Pratt, B.R. (2001):** Oceanography, bathymetry and syn-depositional tectonics of a Precambrian intracratonic basin: integrating sediments, storms, earthquakes and tsunamis in the Belt Super-group (Helena Formation, ca. 1.45 Ga), Western North America: Sedimentary Geology, Vol. 141, pp. 371-394.
- Priezbindowski, D.R. (1985):** Burial cementation is it important? A case study, Stuart City Trend, South-Central Texas. In: N. Schneidermann and P.M. Harris (eds.), Carbonate cement. SEPM spec. Pub. No. 36, pp. 241-264.
- Purdy, E.G. (1968):** "Carbonate diagenesis". An environmental Survey, Geol. Roman 7, pp. 183-228.
- Ragab, M. A., and Ayyad, A. (1985):** Petrophysical and petrographic properties of Nubia sandstone -Core samples from east Oweinat, Egypt. Proc. of 4th Ann. Surv. of Egypt. pp. 280-291.
- Rateb, R. (1988):** Miocene Planktonic foraminiferal analysis and its stratigraphic application in the Gulf of Suez region., 9th E.G.P.C. Exploration and Production Conference, Cairo, Egypt, pp. 275-307.
- Said, R., and El Heiny, I. (1967):** "Planktonic foraminifera from the Miocene rocks of the Gulf of Suez region, Egypt", Cushman contribution from the Cushman foundation V. XVIII. Part I, pp. 14-26.
- Schlumberger Ltd. (1989):** Log interpretation, principle and applications. Schlumberger Wireline & Testing. Sugar Land, Texas, p. 241.
- Selley, R.C. (1996):** Ancient sedimentary environments and their subsurface diagnosis. 4th edition, London, p. 300.
- Serra, O. (1984):** Fundamental of well-log interpretation. Amsterdam-Oxford-New York-Tokyo, p. 250.
- Tromp, S.W. (1949):** The value of Globigerinidae ratios in stratigraphy. J. Paleont. Vol. 23, No. 2, pp. 223-224.
- Tucker, E.M. (2001):** Sedimentary petrology an introduction to the origin of sedimentary rocks. Department of Geological Sciences, University of Durham, Blackwell publications, 3rd ed. pp. 62-65.
- Turner, P. (1980):** The diagenesis of continental red beds. In: Turner, P. (ed.) Continental Red Beds: Development in Sedimentology. Elsevier, Amsterdam, p. 562.

- Waite, S.T., and Pooley, R.W. (1953):** Report on the Nukhul Formation. Egyptian General Petroleum Company (E.G.P.C), Internal report (G.R. 422).
- Walker, T.R., Waugh, B., and Grone, A.J. (1978):** Diagenesis in first cycle desert alluvium of Cenozoic age, southwest United States and Northwest Mexico. Geol. Soc. Amer. Bull., 89, pp. 19-32.
- Wood, J.R. (1989):** Modeling the effect of compaction and precipitation/dissolution on porosity. In: Hutcheon. I.E. (ed.) Burial Diagenesis. Mineral. Assoc. of Canada Short Course 15, pp. 311-362.
- Zenger, D.H. (1973):** Syntaxial calcite borders on dolomite crystal. Little Falls, Jour. Sed. Petrol., Vol. 43, pp. 118-124.